Charmaine Toy
Automation Engineer,
DiCon Fiberoptics, Inc.,
Richmond, CA 94804
e-mail: charm@calalumni.org

Luis Alvarez
Professor,
Instituto de Ingenieria,
Universidad Nacional Autònoma de México,
Mexico City, Mexico
e-mail: alvar@pumas.iingen.unam.mx

Roberto Horowitz
Professor,
Department of Mechanical Engineering,
University of California at Berkeley,
Berkeley, CA 94720
e-mail: horowitz@me.berkeley.edu

Nonstationary Velocity Profiles for Emergency Vehicles on Automated Highways

This paper explores the notion and usefulness of nonstationary velocity profiles for high priority emergency vehicle transit on automated highways. These profiles are intended for use in the link layer of the hierarchical control architecture defined by the California Partners for Automated Transit and Highways (PATH) program. A non-stationary velocity profile which can be used to circulate traffic around a faster moving emergency vehicle is introduced. The effects on traffic flow are illustrated. A traffic flow controller that sustains nonstationary velocity profiles on fully automated highways is designed. Controller stability is discussed stressing the usefulness of nonstationary velocity profiles in creating a moving area of low vehicle density. Simulation results obtained using SmartCap, a traffic flow simulation program, demonstrate the fast circulation of an emergency vehicle in AHS while high traffic flow is maintained. [DOI: 10.1115/1.1434981]

1 Introduction

The design of Automated Highway Systems (AHS) under the hierarchical control structure described in [1] consists of five hierarchical layers: network, link, coordination, regulation and physical (see Fig. 1). The first two layers are roadside control systems, and the latter three are installed on each automated vehicle. One network layer controller exists for the entire automated highway network, which assigns routes such that vehicles minimize a given measure of performance, such as travel time. Network layer control is exerted by specifying a desired traffic flow profile in each of the highway junctions. A single link layer controller supervises several links or highway sections. Each highway section is approximately 100 to 500 m long. The link layer does not identify individual vehicles, but rather specifies velocities, platoon size and lane changing for each particular vehicle type or destination. Roadside sensors provide vehicle count information for each link. Control commands from the link layer are transmitted to the lower control layers residing in each vehicle that carry out the prescribed maneuvers, while maintaining safety at all times. The coordination layer [2–4] determines what maneuvers to perform, manages inter-vehicle communications, and coordinates the movement of the vehicle with neighboring cars. The regulation layer, a continuous-time feedback controller, receives commands from the coordination layer and executes the chosen maneuvers [5–7]. The lowest hierarchical level is the physical layer, which pertains to the vehicle's dynamics. It receives steering, throttle, and brake actuator commands from the regulation layer and returns information such as vehicle speed, acceleration, and engine state.

Work performed in this paper pertains to controller design for the link layer. Link layer commands (velocity and proportions of vehicles changing lane) are transmitted to the coordination layer controllers on each individual vehicle on the AHS. Each vehicle on a highway link attempts to adjust its activities to match the transmitted commands; whether commands are executed is dependent on the vehicle's current state and safety requirements. For example, a vehicle may not be able to achieve the link layer velocity because of a slower moving vehicle downstream, or it may exceed the link layer velocity while involved in a specific maneuver, such as joining a platoon. Because safe capacity constraints [8] on the AHS are guaranteed, the link layer control laws here presented are such that the real AHS vehicle velocity and proportions of vehicles changing lane will agree on average with the commands transmitted from the link layer controller.

The link layer controller is comprised of feedforward and stabilizing portions (see Fig. 2). The feedforward controller specifies desired highway flow trajectories, which match fluctuating highway capacity conditions. The stabilizing controller provides feedback action for the traffic flow to match the desired trajectory. This paper discusses the design of the non-stationary velocity profile for the feedforward controller and presents feedback controllers that cope with time-varying feedforward velocity profiles. These feedback controllers are different from those presented in [9] and [10] because now they do not require the feedforward controller to specify stationary velocity profiles that depend only on vehicles' location and not upon time. Non-stationary velocity profiles are useful for changing local traffic behavior without impact to the capacity of entire AHS. Examples of applicable scenarios include emergency vehicles circulating on the AHS or decreasing local vehicle density in a given time and location so that lane change maneuvers can be performed. The controllers are demonstrated in simulation for the high priority transit of an emergency vehicle.

2 Modeling and Notation

The link layer flow is modeled by a set of partial differential equations based on a conservation of vehicles principle. Vehicle density, K, is expressed in *cars/m* and parameterized by time (t), lane, and longitudinal highway position (x). Time and spatial dependencies are implicit in the notation except where noted.

- $\mathbf{K}(t,x)=[K_1 K_2 \ldots K_m]^T$, vector of vehicle densities in lanes 1 through m
- $\mathbf{V}(t,x)=\mathrm{diag}(V_1,V_2,\ldots,V_m)$, diagonal matrix of vehicle velocities in lanes 1 through m

Contributed by the Dynamic Systems and Control Division for publication in the JOURNAL OF DYNAMIC SYSTEMS, MEASUREMENT, AND CONTROL. Manuscript received by the Dynamic Systems and Control Division May 18, 2000. Associate Editor: S. Sivashankar.

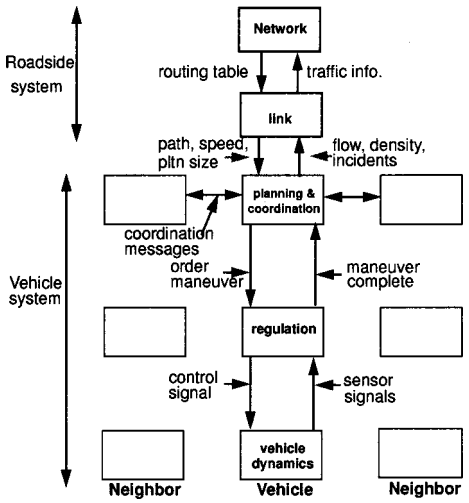

Fig. 1 PATH hierarchical control architecture

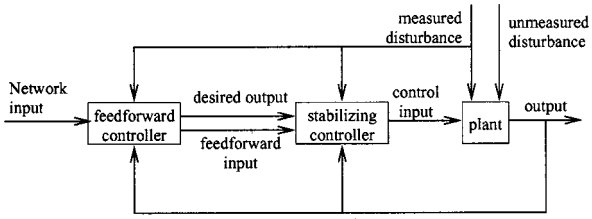

Fig. 2 Link layer controller

$$\bullet\,\mathbf{N}(t,x)=\begin{bmatrix} -n_{1,2} & n_{2,1} & \cdots 0 \\ n_{1,2} & -n_{2,1}-n_{2,3} & \cdots 0 \\ 0 & n_{2,3} & \cdots 0 \\ & \vdots & \\ 0 & \cdots & -n_{m,m-1} \end{bmatrix},$$

where $n_{i,j}(t,x)$ is the proportion of vehicles changing lane from lane i to j per unit time. These proportions apply only to vehicles at position x and time t.

Subscripts of t and x denote partial derivatives with respect to those variables. In this paper modeling framework, vehicle destination is not differentiated, and only two types of vehicles are considered: those with and without high transit priority. The framework, however, can be expanded to do so [11]. The conservation of vehicles principle is expressed as

$$\mathbf{K}_t=-[\mathbf{VK}]_x+\mathbf{NK} \tag{1}$$

Physical highway constraints impose certain conditions on the variables involved: namely, $V_i \geqslant 0$ for all lanes $i=1\ldots m$ and $n_{j,k}\geqslant 0$ for all adjoining lanes j and k. A desired traffic flow behavior is introduced and it is assumed that it also obeys a conservation law for vehicles; the desired traffic flow behavior should also be physically realizable. Subscript d refers to desired traffic flow behavior.

$$[\mathbf{K}_d]_t=-[\mathbf{V}_d\mathbf{K}_d]_x+\mathbf{N}_d\mathbf{K}_d \tag{2}$$

$\mathbf{K}_d$, $\mathbf{V}_d$, and $\mathbf{N}_d$ are associated with the link layer feedforward control. The design of a link layer traffic flow controller consists of 1) specification of desired traffic flow behavior for the feedforward link layer controller and of 2) an appropriate stabilizing feedback control law which minimizes an error norm for the difference between the actual and desired traffic flow behavior.

3 Nonstationary Velocity Profiles

A nonstationary velocity profile is defined to be a velocity function which moves with a determined speed. Figure 3 shows an example of a nonstationary velocity profile for a single lane. The graph depicts the traffic speed versus highway coordinate at a particular time. The shape shown in the figure travels along the highway at specified speed, $w(t)$ and does not change as it moves on the highway. In this paper, nonstationary velocity profiles are parameterized by a single coordinate s as shown in Eq. (3), which defines the new spatial coordinate in terms of the original coordinates x and time t. The function $w(\cdot)$ describes the profile's propagation speed.

$$s=x-\int_0^t w(\varepsilon)d\varepsilon \tag{3}$$

In this section it is shown that nonstationary velocity profiles can be utilized to produce circulating regions of low vehicle density. The nonstationary velocity profile of Fig. 3 has a speed of $w(t)$, which is greater than that of any highway vehicle. Vehicles in each of the highway sections travel at speeds specified by the velocity profile at a given location and time. To determine the associated changes in density due to this velocity profile under steady state conditions, the time derivative of the integral $\int_a^b K_d dx$ is evaluated in the region $[a,b]$.

$$\frac{d}{dt}\int_a^b K_d dx=\dot{b}K_d(t,b)-\dot{a}K_d(t,a)+\int_a^b [K_d]_t dx \tag{4}$$

For a steady-state solution, set the derivative of the left-hand side of Eq. (4) to zero and utilize Eq. (2) to obtain an expression that relates the densities at locations a and b to each other, after and before encountering the velocity profile, respectively.

$$K_d(t,a)=\frac{\dot{b}-V_d(t,b)}{\dot{a}-V_d(t,a)}K_d(t,b) \tag{5}$$

If the velocity profile does not change shape and travels faster than all vehicles at speed, $w(t)$, then let $w(t)=\dot{a}=\dot{b}>V_d(t,x)\forall x,\ t$. It can be noted from Fig. 3 that $V_d(t,b)>V_d(t,a)$ and, thus, that $K_d(t,a)<K_d(t,b)$ from Eq. (5). The nonstationary velocity profile creates a region of low vehicle density which coincides with the dip in velocity in Fig. 3.

The traveling region of low vehicle density can also been seen in an approximate time-space (TS) diagram in Fig. 4 for the velocity profile. On this plot of highway distance versus time, the trajectories of many highway vehicles are depicted. Each line represents the path of a single vehicle. At $t=0s$, vehicles are spaced every 100 m and travel at 20 m/s, which is the initial slope. The velocity profile travels at 30 m/s. When vehicles encounter the profile, they slow to 10 m/s, which is reflected in the decrease in slope. After exiting the profile, vehicles return to their initial slope/speed of 20 m/s. To observe the effects of the velocity profile, focus on the highway section between 7000 m and 7500 m. At $t=40$ s, there are 6 vehicles in this section of highway (inclusive). During the traffic slowdown at $t=100$ s to 10 m/s there are

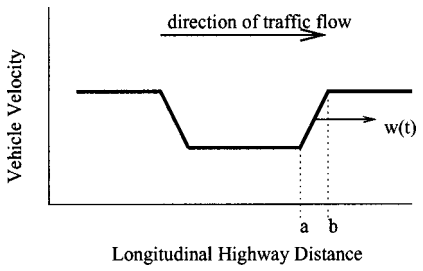

Fig. 3 One lane nonstationary velocity profile

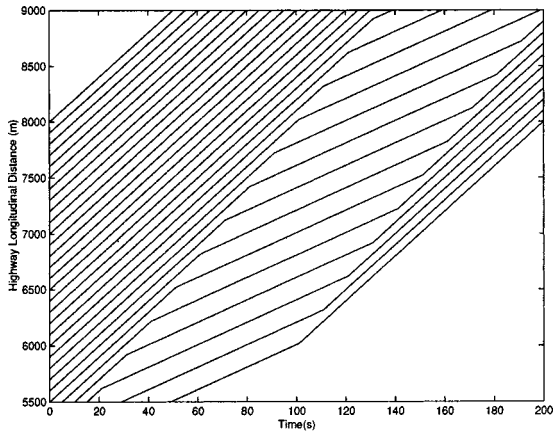

Fig. 4 Time space diagram for Fig. 3

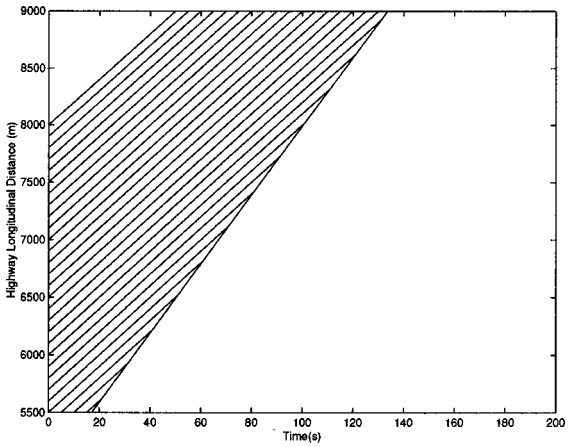

Fig. 6 Time space diagram for Fig. 5

only 3 vehicles in the same section. The vehicle density returns to 6 vehicles after the velocity wavelet passes. It can be seen that the velocity profile produces an accompanying region of low-vehicle density.

These regions of low vehicle density can be desirable from a safety standpoint; they allow vehicles inside the regions more time and opportunity to perform maneuvers such as lane changing under decreased traffic density conditions. Slower moving vehicles require less headway space for safety. A moving region of low vehicle density, which results from the nonstationary velocity profile, can be used to perform vehicle maneuvers which are otherwise not possible due to capacity and safety constraints.

Depending on shape and traveling speed, velocity profiles can also lead to point accumulations of vehicles and can have a detrimental effect on traffic. Figure 5 illustrates a single lane example. In this case $w(t)=\dot{a}=\dot{b}=V_d(t,a)>V_d(t,b)$. Eq. (5) implies an infinite increase in the vehicle density, $K_d(t,a)$. Slower moving vehicles in front of $x=a$ are caught up by the rapidly moving velocity profile traveling at $w(t)$. Once a vehicle's position coincides with point a, its velocity becomes the same as that of the velocity profile, $w(t)$; the vehicle is forced to travel with the velocity profile, which accumulates the slower moving vehicles in front of it.

Figure 6 depicts the approximate TS diagram for this unstable velocity profile. At $t=0\,s$, vehicles are spaced every $100\,m$ and travel at $20\,m/s$. The profile travels at $30\,m/s$. As vehicles encounter the traveling velocity profile from behind, they speed up to $30\,m/s$, which is shown as an increase in the slope of each trajectory. At the lower boundary of the graph, all the vehicles join together in a single path, which corresponds to an accumulation of vehicle density along the trajectory. This can be thought of as vehicles joining the velocity profile as it moves along the highway and those cars being unable to escape the profile. Because the profile overtakes all cars and retains them, the number of vehicles inside the profile increases indefinitely.

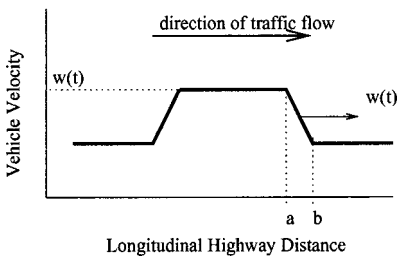

Fig. 5 One lane nonstationary velocity profile

If there is more than one highway lane, this accumulation of vehicles can be cancelled by use of lane changes. Lane changes are utilized in front of the point of accumulation, where $V_d(t,a)=w(t)$, to empty the lane of vehicles so that they are not caught up in the shock wave. The vehicles that change lane can be returned to the original lane after the wave has passed. For safety considerations and spacing requirements, lane changing should not occur between lanes with a large difference in speed at that location.

Figure 7 shows a set of velocity profiles for two lanes which utilize lane changing. The two profiles travel together at speed $w(t)$, which is equal to the maximum speed in lane 1, $w(t)=V_{\text{high}}$. The overall number of vehicles on the AHS is high, such that vehicles in both lanes cannot be moved into a single lane while maintaining the nominal speed due to safe spacing constraints. As vehicles in both lanes encounter the velocity profile, the vehicles decelerate to V_{low}. The deceleration has the same effect as illustrated in the case shown in Fig. 3, i.e., vehicle density decreases in the location of V_{low} by the proportion given in Eq. (5). This slow speed vehicle density region can be utilized for lane changing. The velocity profile is defined such that the velocity of vehicles at $x=x_e$ is V_{high}, the maximum speed of lane 1. In this particular case, the speed of the velocity profile is set by design to be $w(t)$. Because $V_{\text{high}}=w(t)$ at $x=x_e$, any vehicles which remain in lane 1 will be caught up in the shock wave if not moved out of the way, as illustrated in Fig. 5. The velocity profile's characteristics at $x=x_e$ are the same as that of the example shown in Fig. 5, which experiences a point accumulation of vehicles. It is necessary to determine the proportion of vehicles that

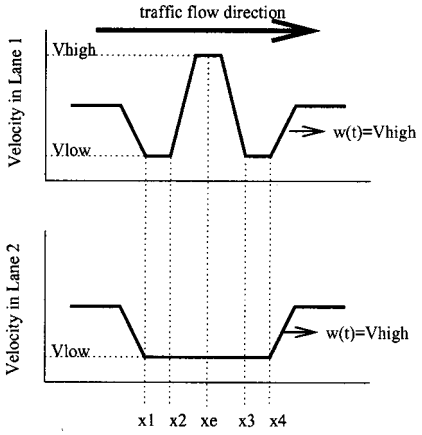

Fig. 7 Two lane nonstationary velocity profiles

need to change lane out of lane 1 and into lane 2. For safety reasons, vehicles are allowed to change lane only in regions where both lanes have the same highway speed. Assume that

$$n_{d,1,2}(t,x)\neq 0 \quad x\in[x_3,x_4]$$
$$n_{d,2,1}(t,x)=0 \tag{6}$$

The link layer controllers attempt to move all vehicles out of the way; i.e., $K_{d,1}(t,x_3)=0$. Using Eq. (4) together with Eq. (2), we obtain:

$$\frac{d}{dt}\int_{x_3}^{x_4}K_{d,1}dx = V_{high}[K_{d,1}(t,x_4)-K_{d,1}(t,x_3)]+\int_{x_3}^{x_4}-[V_{d,1}K_{d,1}]_x - n_{d,1,2}K_{d,1}dx$$
$$=(V_{high}-V_{low})K_{d,1}(t,x_4)-\int_{x_3}^{x_4}n_{d,1,2}K_{d,1}dx \tag{7}$$

For a steady-state solution without accumulation of vehicles in $x\in[x_3,x_4]$, set the left hand side of Eq. (7) to zero. Assuming that the proportion of vehicles changing lane per unit time in this interval is constant, Eq. (8) is obtained. $\int_{x_3}^{x_4}K_{d,1}dx$ is the number of vehicles between x_3 and x_4. In the case of no vehicles, we can safely set $n_{d,1,2}(t,x)=0$ for $x\in[x_3,x_4]$.

$$n_{d,1,2}(t,x)=\frac{[V_{high}-V_{low}]K_{d,1}(t,x_4)}{\int_{x_3}^{x_4}K_{d,1}dx} \quad x\in[x_3,x_4] \tag{8}$$

If vehicles are not able to change lane out of the way in response to the link layer commands due to safety conditions (e.g., another vehicle alongside), special coordination layer maneuvers have been developed to circulate vehicles out of the way [12]. The link layer works together with the coordination layer to prevent the accumulation of vehicles.

For $x<x_e$ in Fig. 7, lane 1 is void of vehicle density because of the lane changing downstream $x\in[x_3,x_4]$. To describe the return of vehicles to lane 1, a similar expression is derived for lane 2 for $x\in[x_1,x_2]$. It is assumed that the following holds true for the proportions of lane changing.

$$n_{d,2,1}(t,x)\neq 0 \quad x\in[x_1,x_2]$$
$$n_{d,1,2}(t,x)=0 \tag{9}$$

In a similar manner to deriving Eq. (8), Eq. (4) is combined with Eq. (2) to obtain

$$\frac{d}{dt}\int_{x_1}^{x_2}K_{d,2}dx = V_{high}[K_{d,2}(t,x_2)-K_{d,2}(t,x_1)]+\int_{x_1}^{x_2}-[V_{d,2}K_{d,2}]_x - n_{d,2,1}K_{d,2}dx$$
$$=(V_{high}-V_{low})[K_{d,2}(t,x_2)-K_{d,2}(t,x_1)] - \int_{x_1}^{x_2}n_{d,2,1}K_{d,2}dx \tag{10}$$

This expression differs from Eq. (7) because the number of vehicles to retain in lane 2 after the velocity profile has passed, $K_{d,2}(t,x_1)$ can be chosen. For a steady-state solution, set the left hand side of Eq. (10) to zero and assume that the proportion of vehicles changing lane $n_{d,2,1}$ is constant in the interval $x\in[x_1,x_2]$.

$$n_{d,2,1}=\frac{(V_{high}-V_{low})[K_{d,2}(t,x_2)-K_{d,2}(t,x_1)]}{\int_{x_1}^{x_2}K_{d,2}dx} \quad x\in[x_1,x_2] \tag{11}$$

The denominator of Eq. (11) is the number of vehicles in lane 2 in the interval $x\in[x_1,x_2]$. If there are no vehicles in this region, $n_{d,2,1}$ can be set to zero because there are no cars to control.

Using the velocity profile shown in Fig. 7, a vehicle or priority group of vehicles is able to travel along the highway at speed $w(t)$, faster than the rest of the traffic. The velocity profile indicates that if there is high traffic density on the AHS, the vehicles downstream should decelerate in order to change lane out of the way, which is counterintuitive. The speed and spatial shape of the velocity profile should be chosen such that the maximum acceleration/deceleration capabilities of vehicles is not violated. On a nonautomated highway system, the coordinated deceleration and lane changing needed by the nonstationary velocity profile is difficult to achieve. In future sections, the use of the nonstationary velocity profile will be illustrated and stabilizing traffic flow control laws for an emergency vehicle which must travel faster than the average traffic on an AHS are presented.

4 Traffic Flow Stabilizing Control

A link layer controller does not seek to identify or control individual vehicles; rather, it controls the distribution of vehicle density on the automated highway by issuing speed and activity commands [8]. The link layer controller is comprised of two parts: a feedforward and a stabilizing portion (Fig. 2). The feedforward controller provides a desired traffic flow behavior in terms of vehicle density distribution $\mathbf{K}_d$, traffic flow speed $\mathbf{V}_d$ and activity proportions $\mathbf{N}_d$. An activity that could be described by this type of model is lane changing, for example. The stabilizing controller processes the desired trajectory information and true density distribution to determine feedback control laws for the traffic flow speed and activity proportions. It is assumed that the real traffic flow obeys Eq. (1) and that the desired traffic flow behavior obeys the continuity equation Eq. (2). The trajectory produced by the feedforward controller should be physically meaningful and realizable. Recall that subscript *d* refers to desired traffic.

Control action is exerted by specification of velocity, $\mathbf{V}$, and change lane commands, $\mathbf{N}$, to vehicles along the highway. They are decomposed as

$$\mathbf{V}=\mathbf{V}_d+\mathbf{V}_f,$$
$$\mathbf{N}=\mathbf{N}_d+\mathbf{N}_f \tag{12}$$

where $\mathbf{V}_f$, $\mathbf{N}_f$, $\mathbf{V}_d$, and $\mathbf{N}_d$ represent the feedback and feedforward portions of the controller, respectively. Appropriate choice of the velocity, $\mathbf{V}_f$, and lane change, $\mathbf{N}_f$, feedback terms will be discussed in Section 6. Define the vehicle density error to be $\tilde{\mathbf{K}}=\mathbf{K}_d-\mathbf{K}$. The error dynamics of the traffic density flow are given by Eq. (13).

$$\tilde{\mathbf{K}}_t=-[\mathbf{V}_d\tilde{\mathbf{K}}-\mathbf{V}_f\mathbf{K}]_x+\mathbf{N}_d\tilde{\mathbf{K}}-\mathbf{N}_f\mathbf{K} \tag{13}$$

Previous research for link layer control can be found in [12,11]. In [12], a matrix transformation is utilized to convert vehicle density into a variable which better reflects the influence of velocity fields upon lane change activity. Desired lane change proportions are time-invariant. In [11], a controller without matrix transformation but with time varying lane change proportions is used to demonstrate the stability of the feedback controller. In [13] this controller is used for the circulation of traffic around a moving section of highway. Lane change commands were used to achieve a local region of low vehicle density.

5 Coordinate Transformation

A nonstationary velocity profile is a velocity function parameterized by a single coordinate *s*, as shown in Eq. (14). It is assumed that the velocity profile travels at velocity $w(t)$ and propose the following coordinate transformation for $(x,t)\rightarrow(s,\tau)$ (Eq. (14)).

$$s=x-\int_0^t w(\varepsilon)d\varepsilon$$
$$\tau=t \tag{14}$$

The time and position partial derivatives transform in the following manner:

$$\begin{bmatrix} \frac{\partial}{\partial x} \\ \frac{\partial}{\partial t} \end{bmatrix} = \begin{bmatrix} 1 & 0 \\ -w(t) & 1 \end{bmatrix} \begin{bmatrix} \frac{\partial}{\partial s} \\ \frac{\partial}{\partial \tau} \end{bmatrix} \tag{15}$$

Under this coordinate transformation, Eq. (1) may be rewritten as:

$$[\mathbb{K}]_\tau = -[\mathbb{V}_{rel}\mathbb{K}]_s + \mathbb{N}\mathbb{K} \tag{16}$$

Subscript s refers to partial derivatives with respect to that variable. $\mathbb{K}(\tau,s)$ and $\mathbb{N}(\tau,s)$ are the vehicle density and lane change terms, respectively, after the change of coordinates. The blackboard boldface type refers to matrix quantities in the new coordinate system (τ,s). Eq. (16) describes vehicle densities in the moving coordinate frame in terms of the relative velocity $\mathbf{V}_{rel} \equiv \mathbf{V} - w(t)\mathbf{I}$. The coordinate transformation removes the desired velocity's time dependence and casts the flow equation into a form similar to the original conservation expression (Eq. (1)). The desired traffic flow behavior in Eq. (2) transforms similarly.

$$[\mathbb{K}_d]_\tau = -[\mathbb{V}_{d,rel}\mathbb{K}_d]_s + \mathbb{N}_d\mathbb{K}_d \tag{17}$$

The error dynamics, expressed in the new coordinate system are shown in Eq. (18).

$$[\tilde{\mathbb{K}}]_\tau = -[\mathbb{V}_{d,rel}\tilde{\mathbb{K}}]_s + [\mathbb{V}_f\mathbb{K}]_s + \mathbb{N}_d\tilde{\mathbb{K}} - \mathbb{N}_f\mathbb{K} \tag{18}$$

Because the desired velocity profile travels at speed $w(t)$, the desired relative velocity, $\mathbb{V}_{d,rel}(s) \equiv \mathbb{V}_d(\tau,s) - w(\tau)\mathbb{I}$, is time invariant under the coordinate transformation. It is also assumed that the profile velocity $w(t)$ satisfies $w(t) > V_{i,d}(\tau,s)\ \forall t$, s and for all lanes i. $\mathbb{V}_{d,rel}(s)$ is negative definite $\forall s$.

6 Stabilizing Controller With Matrix Transformation

In this section we present a stabilizing controller based on a matrix transformation for the vehicle error density. This matrix transformation of $\mathbf{K}$ allows to take into account the desired lane change proportions and traffic speed. The matrix transformation varies with relative highway position. Subscripts of t, s and x in this section denote partial differentiation with respect to the variables. Another link layer feedback stabilizing controller that does not require the use of the coordinate transformation is presented in [14,15].

Lemma 1. Let $\mathbb{A}(s)$ *be a nonsingular matrix transformation for the vehicle density* $\tilde{\mathbb{K}}(\tau,s)$ *such that* $\mathbb{A}_s(s) = -\mathbb{A}(s)\mathbb{N}_d(s)\mathbb{V}_{d,rel}^{-1}(s)$. *Define* $\mathbb{G}(\tau,s) \equiv \mathbb{A}(s)\tilde{\mathbb{K}}(\tau,s)$. *Then* $\mathbb{G}_t(\tau,s) = -[\mathbb{A}(s)\mathbb{V}_{d,rel}(s)\mathbb{A}^{-1}(s)\mathbb{G}(\tau,s)]_s + \mathbb{A}(s)[\mathbb{V}_f(\tau,s)\mathbb{K}(\tau,s)]_s - \mathbb{A}(s)\mathbb{N}_f(\tau,s)\mathbb{K}(\tau,s)$.

Proof: Differentiate $\mathbb{G}$:

$$\mathbb{G}_t = \mathbb{A}_t\tilde{\mathbb{K}} + \mathbb{A}\tilde{\mathbb{K}}_t = -[\mathbb{A}\mathbb{V}_{d,rel}\mathbb{A}^{-1}\mathbb{A}\tilde{\mathbb{K}}]_s - \mathbb{A}\mathbb{N}_f\mathbb{K} + \mathbb{A}[\mathbb{V}_f\mathbb{K}]_s \tag{19}$$

■

Lemma 2. Suppose $\mathbb{V}_{d,rel}(s) = \delta\cdot\mathbb{I}$ *and* $\mathbb{A}_s(s) = -\mathbb{A}(s)\mathbb{N}_d(s)\mathbb{V}_{d,rel}^{-1}(s)$. *Then* $\mathbb{G}_t(\tau,s) = -[\mathbb{V}_{d,rel}(s)\mathbb{G}(\tau,s)]_s + \mathbb{A}[\mathbb{V}_f(\tau,s)\mathbb{K}(\tau,s)]_s - \mathbb{A}(s)\mathbb{N}_f(\tau,s)\mathbb{K}(\tau,s)$.

Proof: $\mathbb{A}\mathbb{V}_{d,rel}\mathbb{A}^{-1} = \mathbb{A}\delta\cdot\mathbb{I}\mathbb{A}^{-1} = \mathbb{V}_{d,rel}$. ■

$\mathbb{A}(s)$ is a time independent coordinate transformation and is also required to be nonsingular $\forall s$. Note that $\mathbb{N}_d(s)$ is nonsingular and $\mathbb{V}_{d,rel}(s)$ is nonsingular everywhere. Because of the time independence of $\mathbb{A}(s)$, the matrix can be precomputed a priori. $\mathbb{N}_d(s)$ must also be time independent as well, in order for $\mathbb{A}(s)$ to remain time independent with the dynamics given above.

Theorem 1. Let $\mathbb{V}_{d,rel}(s) = \delta\cdot\mathbb{I}$ *and* $\mathbb{A}_s(s) = -\mathbb{A}(s)\mathbb{N}_d(s)\mathbb{V}_{d,rel}^{-1}(s)$. *Define the velocity feedback law to be* $\mathbb{V}_f(\tau,s) = -\psi(\tau,s)diag\ [\mathbb{A}^T(s)\mathbb{V}_{d,rel}(s)\mathbb{A}(s)\tilde{\mathbb{K}}(\tau,s)]_s$ *and the lane change feedback law to be* $n_{f,i,j} = max[0,\mu(\tau,s) \times (F_i(\tau,s)K_i(\tau,s) - F_j(\tau,s)K_j(\tau,s))]$ *where* $\mathbb{F}(\tau,s) = \mathbb{A}^T(s)\mathbb{V}_{d,rel}(s)\mathbb{A}(s)\tilde{\mathbb{K}}(\tau,s)$. *The boundary conditions are* $\tilde{\mathbf{K}}(0,t) = \tilde{\mathbf{K}}(L,t) = 0$. *Then* L_2 *stability follows.*

Proof: Use the Lyapunov function $W(t) = -1/2\int_0^L \mathbf{G}^T(t,x) \times \mathbf{V}_{d,rel}(t,x)\mathbf{G}(t,x)dx = 1/2\int_{\alpha(t)}^{\beta(t)} \mathbb{G}^T(\tau,s)[-\mathbb{V}_{d,rel}(s)]\mathbb{G}(\tau,s)ds$ where $\alpha(t) = -\int_0^t w(\varepsilon)d\varepsilon$ and $\beta(t) = L - \int_0^t w(\varepsilon)d\varepsilon$. Recall that $\mathbb{V}_{d,rel}$ is negative definite.

$$\begin{aligned} \dot{W}(t) = {} & \frac{1}{2}\beta'(t)\mathbb{G}^T[-\mathbb{V}_{d,rel}]\mathbb{G}\Big|_{s=\beta(t)} - \frac{1}{2}\alpha'(t)\mathbb{G}^T \\ & \times[-\mathbb{V}_{d,rel}]\mathbb{G}\Big|_{s=\alpha(t)} + \frac{1}{2}\int_{\alpha(t)}^{\beta(t)}[\mathbb{G}^T[-\mathbb{V}_{d,rel}]\mathbb{G}]_t ds \\ & - \int_{\alpha(t)}^{\beta(t)} \mathbb{G}^T\mathbb{V}_{d,rel}\mathbb{A}[\mathbb{V}_f\mathbb{K}]_s ds + \int_{\alpha(t)}^{\beta(t)} \mathbb{G}^T\mathbb{V}_{d,rel}\mathbb{A}\mathbb{N}_f\mathbb{K}ds \end{aligned} \tag{20}$$

Using integration by parts and noting that $\mathbb{G}^T\mathbb{V}_{d,rel}[\mathbb{V}_{d,rel}\mathbb{G}]_s = [\mathbb{G}^T\mathbb{V}_{d,rel}]_s\mathbb{V}_{d,rel}\mathbb{G}$.

$$\begin{aligned} \dot{W}(t) = {} & \frac{1}{2}\mathbb{G}^T\mathbb{V}_{d,rel}[\mathbb{V}_{d,rel} + 2w(t)\cdot\mathbb{I}]\mathbb{G}\Big|_{\alpha(t)}^{\beta(t)} - [\mathbb{G}^T\mathbb{V}_{d,rel}\mathbb{A}\mathbb{V}_f\mathbb{K}]_{\alpha(t)}^{\beta(t)} \\ & + \int_{\alpha(t)}^{\beta(t)}[\mathbb{G}^T\mathbb{V}_{d,rel}\mathbb{A}]_s\mathbb{V}_f\mathbb{K}ds + \int_{\alpha(t)}^{\beta(t)}\mathbb{G}^T\mathbb{V}_{d,rel}\mathbb{A}\mathbb{N}_f\mathbb{K}ds \end{aligned} \tag{21}$$

Impose the conditions that $\mathbf{V}_f(t,x=0) = \mathbf{V}_f(t,x=L) = 0$.

$$\dot{W}(t) = \frac{1}{2}\mathbb{G}^T\mathbb{V}_{d,rel}[\mathbb{V}_{d,rel} + 2w(t)\cdot\mathbb{I}]\mathbb{G}\Big|_{\alpha(t)}^{\beta(t)} \tag{22}$$

$$+ \int_{\alpha(t)}^{\beta(t)}[\mathbb{G}^T\mathbb{V}_{d,rel}\mathbb{A}]_s\mathbb{V}_f\mathbb{K}ds + \int_{\alpha(t)}^{\beta(t)}\mathbb{G}^T\mathbb{V}_{d,rel}\mathbb{A}\mathbb{N}_f\mathbb{K}ds \tag{23}$$

Recall that $\mathbb{F}(\tau,s) \equiv \mathbb{A}^T(s)\mathbb{V}_{d,rel}(s)\mathbb{A}(s)\tilde{\mathbb{K}}(\tau,s)$.

$$\int_{\alpha(t)}^{\beta(t)}[\mathbb{G}^T\mathbb{V}_{d,rel}\mathbb{A}]_s\mathbb{V}_f\mathbb{K}ds = \int_{\alpha(t)}^{\beta(t)} -\psi(\tau,s)\sum_i K_iF_i^2 ds \leq 0 \tag{24}$$

$$\begin{aligned} \int_{\alpha(t)}^{\beta(t)}\mathbb{G}^T\mathbb{V}_{d,rel}\mathbb{A}\mathbb{N}_f\mathbb{K}ds &= \int_{\alpha(t)}^{\beta(t)}\mathbb{F}^T\mathbb{N}_f\mathbb{K}ds \\ &= \int_{\alpha(t)}^{\beta(t)}\sum_{\substack{i\neq j=1 \\ |i-j|\leq 1}}^{m} -\mu(\tau,s)(F_jK_j - F_iK_i)^2 \\ &\leq 0 \quad \forall\mu(\tau,s) \geq 0 \end{aligned} \tag{25}$$

$$\begin{aligned} \dot{W}(t) &\leq \frac{1}{2}\mathbb{G}^T\mathbb{V}_{d,rel}[\mathbb{V}_{d,rel} + w(t)\cdot\mathbb{I}]\mathbb{G}\Big|_{\alpha(t)}^{\beta(t)} \\ &\leq \frac{1}{2}\mathbb{G}^T\mathbb{V}_{d,rel}\mathbb{V}_d\mathbb{G}\Big|_{\alpha(t)}^{\beta(t)} \leq 0 \end{aligned} \tag{26}$$

where $\mathbb{V}_{d,rel}(s) < 0$ and $\mathbb{V}_d(\tau,s) > 0$. ■

7 Simulation Results

The feedforward and feedback controllers described in the previous sections are applied to control the circulation of an EV in an AHS. High priority transit is desired for the EV, which should move faster than the surrounding traffic. From a safety standpoint, an area of low vehicle density is desired around the moving EV so that other vehicles can circulate around it. This region of low vehicle density is achieved by moving a low velocity profile in the non-EV lane, as discussed in Section 3. In the EV lane, vehicles

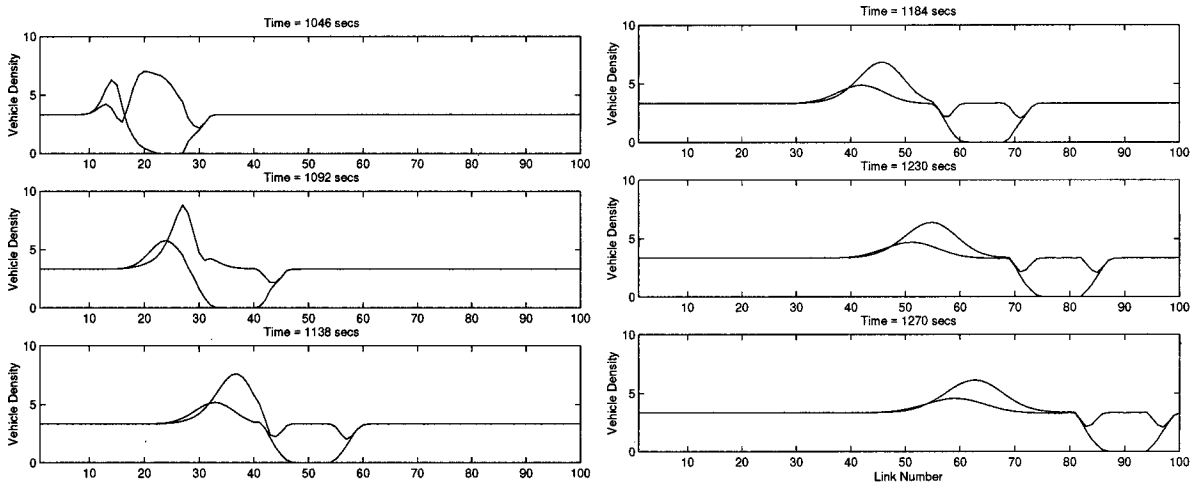

Fig. 8 No feedback control: vehicle density versus longitudinal section

are requested to move out of the way; these vehicles must also decrease speed to provide safe lane changing space. The nonstationary velocity profile to be used is shown in Fig. 7. The EV travels at the location of the peak velocity in lane 1. To avoid vehicle pile-up in front of the EV and to restore the nominal flow of the highway after the EV passes, lane changing is required.

SmartCap [16], a traffic flow simulation package, is used to simulate a hypothetical emergency vehicle (EV) circulating on a two lane highway. The controller with coordinate transformation described in Section 6 is used for feedback control.

In these simulations, all vehicles are assumed independent (i.e., no platoons) and all highway sections are 100 m long. A safety policy which imposes constraints on vehicle spacing dependent on activity and vehicle speed is imposed. Activities such as changing lane require additional space in both the origin and destination lanes.

In Figs. 8 and 9, SmartCap results are shown for the two lane nonstationary profile without control feedback. At $t=0$, the highway is empty and a net inflow of 4800 vehicles per hour distributed equally over the lanes is allowed. These vehicles travel at the nominal speed of 20 m/s. By $t=1000\,s$, the highway is filled evenly with 3.3 vehicles per section. At this time the velocity profile is formed and begins to travel at 30 m/s. The vehicles inside the profile decelerate to 10 m/s in order to change lane out of the way of the EV.

It is important to note that vehicles at the nominal velocity of 20 *m/s* cannot change lane out of the way of the EV while maintaining that speed due to capacity constraints. The time delay between its deceleration and that of the car in front causes vehicles to ''spread out.'' In this low density region, vehicles are then able to change lane out of the EV's lane. While the adjacent lane's vehicles continue to travel at 10 m/s, the EV travels along with the velocity profile at 30 m/s. After the EV has passed, vehicles in the adjacent lane are able to change lane back into the EV lane while maintaining the slow speed of 10 m/s. Vehicles in both lanes then accelerate to the nominal traffic speed upon leaving the nonstationary velocity profile. Highway capacity conditions do not permit all vehicles to change lane into a single lane at the speed of 30 m/s. At lower speeds, headway space demands can be relaxed. The nonstationary velocity profile allows fast circulation of local traffic around an emergency vehicle without restriction of highway inflow.

In Fig. 9 the velocity profile retains the basic shape shown in Fig. 7 in the absence of feedback. This is due to the fact that the

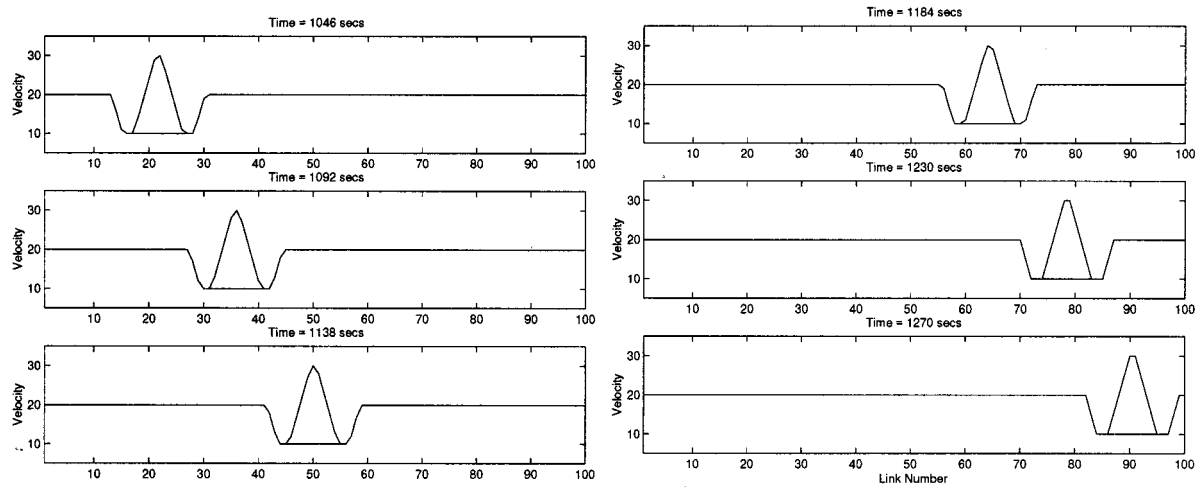

Fig. 9 No feedback control: vehicle velocity versus longitudinal section

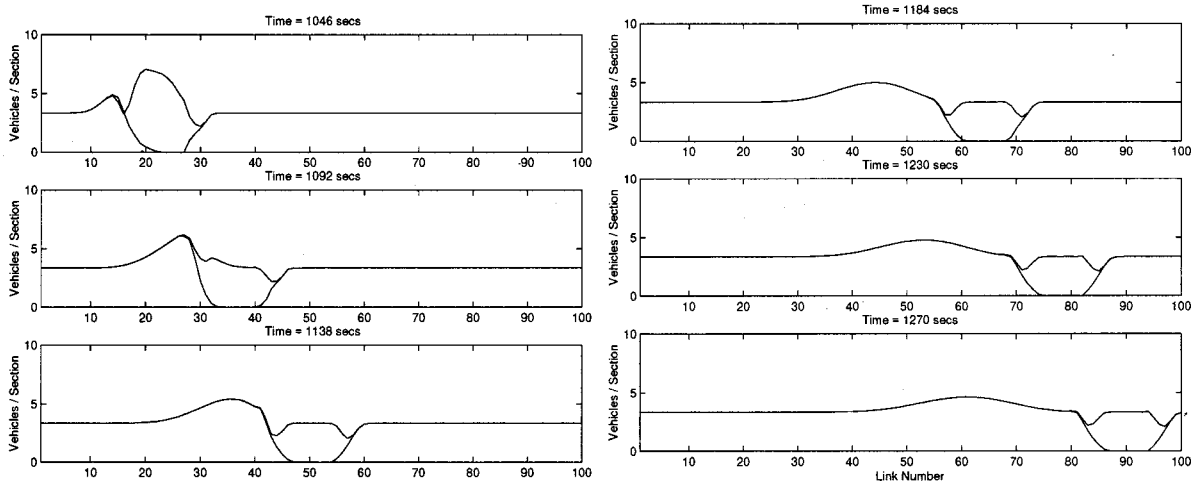

Fig. 10 Feedback control: vehicle density versus longitudinal section

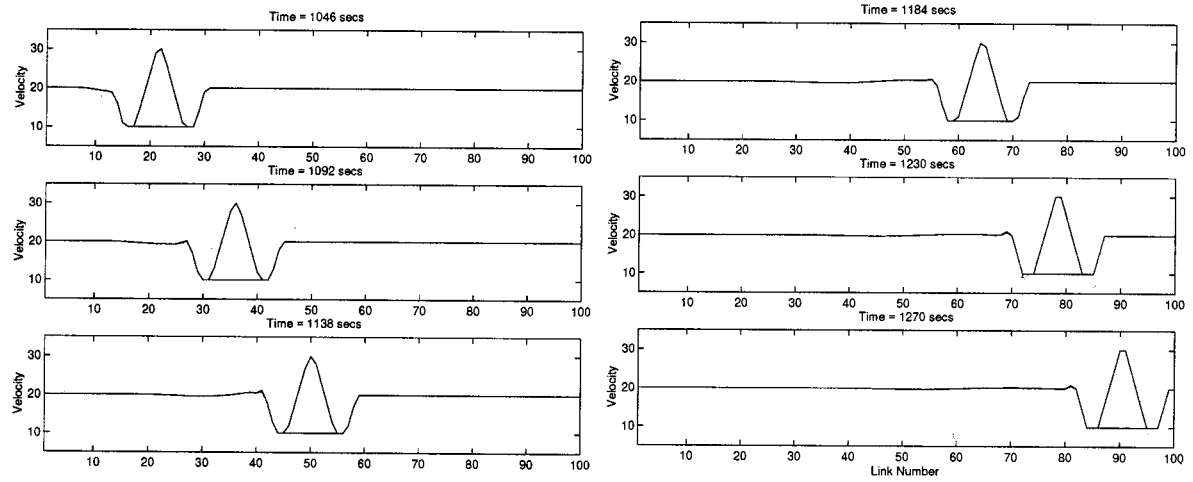

Fig. 11 Feedback control: vehicle velocity versus longitudinal section

commands sent to the highway vehicles are entirely based upon the desired traffic profile ($N=N_d$ and $V=V_d$), which are specifically designed to generate the density distribution shown in Fig. 7. However, there are differences between Fig. 7 and Fig. 9; a pile-up of vehicle density results upstream of the profile in Fig. 9 because vehicles must be moved out of the way to create space for the EV. In the absence of feedback control, this pile-up persists during the simulation and travels down the highway at the nominal speed. When space for the EV is initially formed in lane 1, vehicles must change lane into lane 2. Because the vehicles do not return to their original lane 1, there is a greater pile-up of vehicle density in lane 2 than in lane 1 upstream.

Figures 10 and 11 depict the results of a simulation with the same highway conditions but utilizing the coordinate transformation controller of Section 6 for feedback. Prior to simulation, the matrix transformation, $\mathbb{A}(s)$ is precomputed in Matlab. The overall effect of the feedback control is a smoother vehicle density distribution. After the initial formation of space for the EV, the peak number of vehicles in a section is greater in the absence of feedback control, resulting in greater perturbation.

The pile-up of vehicle density upstream of the profile is dissipated as time progressed due to feedback control. The velocity profile shown in Fig. 11 is similar in general shape to Fig. 9 except for a slight ''bowing'' of the velocity curve where the pile-up is located. Very small changes in the velocity curve result in significant vehicle density dissipation. This suggests that using control feedback for dissipation of local density peaks may have little negative impact on large scale highway capacity. The vehicle density is also equalized in the two lanes upstream of the profile due to lane change feedback. The amount of lane changing activity behind the profile is significant. Restoration of nominal highway conditions behind the EV is desirable from a capacity standpoint. Simulations utilizing the controller in [14,15] produce similar results.

8 Conclusions

Link layer traffic flow controllers to be used within the PATH hierarchical control architecture are introduced. Nonstationary velocity profiles for multilane highways that include changes in vehicles speed and lane are described. By analyzing the effects of shape and speed of these profiles on the traffic flow, it is determined that they create a moving region of low density. This region, that can be moved with a speed greater than the maximum vehicle speed, allows the fast circulation of emergency vehicles, a very important feature for incident handling inside or outside the AHS. Implementing this non-stationary velocity profiles requires

communication and coordination among vehicles to anticipate induced disturbances. For this reason these profiles may not be feasible for manual traffic highways.

A traffic flow controller that is capable of stabilizing the nonstationary velocity profiles is presented. This controller differs from previous work [12,9] in that the desired velocity profile is allowed to vary in time, a very important feature when dealing with emergency or incident maneuvers in AHS. As a result, maneuvers can be safely executed while high vehicle density is maintained everywhere else on the AHS. Simulation results illustrate the performance of the controller.

Acknowledgments and Disclaimer

The work presented in this paper was supported by the California Partners for Automated Transit and Highways (PATH) under project MOU-311. The contents of this paper reflect the views of the authors and do not necessarily reflect the official policies of California PATH. The paper does not constitute a standard, specification or regulation.

References

[1] Varaiya, P., 1993, ''Smart Cars on Smart Roads: Problems of Control,'' IEEE Trans. Autom. Control, **AC-38**, No. 2, pp. 195–207.

[2] Horowitz, R., and Varaiya, P., 2000, ''Control Design of an Automated Highway System,'' Proceedings of the IEEE: Special Issue on Hybrid Systems, **88**, No. 7, pp. 913–925, July.

[3] Rao, B., and Varaiya, P., 1993, ''Roadside Intelligence for Flow Control in IVHS,'' Technical report, PATH, University of California at Berkeley, Aug.

[4] Hsu, A., Eskafi, F., Sachs, S., and Varaiya, P., 1994, ''Protocol Design for an Automated Highway System,'' Discrete Event Dynamic Systems, **2**, No. 1, pp. 4–16.

[5] Li, P. Y., Alvarez, L., and Horowitz, R., 1997, ''AHS Safe Control Laws for Platoon Leaders,'' IEEE Trans. on Control Syst. Technol., **5**, No. 6, pp. 614–628, Nov.

[6] Alvarez, L., and Horowitz, R., 1999, ''Safe Platooning in Automated Highway Systems. Part I: Safety Regions Design,'' Veh. Syst. Dyn., **32**, No. 1, pp. 23–56, July.

[7] Alvarez, L., and Horowitz, R., 1999, ''Safe Platooning in Automated Highway Systems. Part II: Velocity Tracking Controller,'' Veh. Syst. Dyn., **32**, No. 1, pp. 57–84, July.

[8] Broucke, M., and Varaiya, P., 1996, ''A Theory of Traffic Flow in Automated Highway System,'' Transportation Research, Part C: Emerging Technologies, **4**, No. 4, pp. 181–210.

[9] Alvarez, L., Horowitz, R., and Li, P., 1997, ''Traffic Flow Control in Automated Highway Systems,'' *Proceedings of the 8th IFAC Symposium on Transportation Systems*, Chania, Greece, June.

[10] Toy, C., Alvarez, L., and Horowitz, R., 2001, ''Multidestination Traffic Flow Control in Automated Highway Systems,'' accepted for publication in Transportation Research Part C: Emergent Technologies.

[11] Alvarez, L., Horowitz, R., and Li, P., 1999, ''Traffic Flow Control in Automated Highway Systems,'' Control Engineering Practice, **7**, No. 11, pp. 1071–1078.

[12] Li, P., Horowitz, R., Alvarez, L., Frankel, J., and Roberston, A., 1997, ''An AHS Link Layer Controller for Traffic Flow Stabilization,'' Transportation Research, Part C: Emerging Technologies, **5**, No. 1, pp. 11–37.

[13] Toy, C., Leung, K., Alvarez, L., and Horowitz, R., 1998, ''Emergency Vehicle Maneuvers and Control Laws for Automated Highway Systems,'' *Proceedings of the 1998 ASME International Mechanical Engineering Congress and Exposition. Anaheim, CA*, Nov.

[14] Toy, C., Alvarez, L., and Horowitz, R., 1999, ''A Traffic Flow Controller for Non-stationary Velocity Profiles on Automated Highway,'' *Proceedings of the 1999 ACC*, pp. 3691–3696.

[15] Toy, C., 2000, ''Emergency Vehicle Maneuvers and Control Laws for Automated Highway Systems,'' PhD thesis, Department of Mechanical Engineering, University of California at Berkeley.

[16] Broucke, M., Varaiya, P., Kourjankski, M., and Khorramabadi, D., 1998, SmartCap User's Guide, Technical report, Department of Electrical Engineering and Computer Science, University of California, Berkeley, California, May.